

# Anomalous quantum reflection of Bose-Einstein condensates from a silicon surface: the role of dynamical excitations

R.G. Scott<sup>1</sup>, A.M. Martin<sup>2</sup>, T.M. Fromhold<sup>1</sup> and F.W. Sheard<sup>1</sup>

<sup>1</sup>*School of Physics and Astronomy, University of Nottingham,  
Nottingham NG7 2RD, United Kingdom*

<sup>2</sup>*School of Physics, University of Melbourne, Parkville, Vic. 3010, Australia*

(December 2, 2024)

We investigate the effect of inter-atomic interactions on the quantum-mechanical reflection of Bose-Einstein condensates from regions of rapid potential variation. The reflection process depends critically on the density and incident velocity of the condensate. For low densities and high velocities, the atom cloud has almost the same form before and after reflection. Conversely, at high densities and low velocities, the reflection process generates solitons and vortex rings that fragment the condensate. We show that this fragmentation can explain the anomalously low reflection probabilities recently measured for low-velocity condensates incident on a silicon surface.

PACS numbers: 34.50.Dy 03.75.Kk 03.75.Lm

Advances in atom cooling and trapping have enabled the exploration of diverse quantum transport and interference effects for both individual atoms [1] and Bose-Einstein condensates (BECs) [2–15]. In BECs, inter-atomic interactions can cause complex collective excitations of the atom cloud, such as soliton and vortex formation [8–10], and dynamical and Landau instabilities [11,12,16], which strongly influence the BEC’s center-of-mass motion. There is great current interest in using condensed matter systems to provide new tools for manipulating ultra-cold atoms, for example micron-scale current-carrying wires on a semiconductor surface [17]. Understanding and controlling the interactions between the atoms and the surface is of crucial importance for the development of these “atom chips”. Recent experimental studies of Na-atom BECs bouncing off a Si surface provide a powerful probe of such interactions [13]. When the approach velocity is low, the rapid variation of the surface potential causes quantum-mechanical reflection of the atom cloud. In the experiments [13], the fraction of the BEC that undergoes quantum reflection was measured as a function of the incident velocity,  $v_x$ . Although quantum-mechanical calculations predict that the reflection probability for a *single* atom will increase monotonically as  $v_x$  decreases [13,14], the measured reflection probability for the BEC *decreases* with decreasing  $v_x$  below  $\sim 1.7$  mm s $^{-1}$ : an interesting observation that is not yet understood [13].

In this Letter, we show that inter-atomic interactions can have a pronounced effect on the quantum reflection of BECs from Si surfaces, consistent with the anomalously low reflection probabilities observed in experiment [13]. Our results demonstrate that the underlying physics is a *generic* feature of the reflection of BECs from regions of rapid potential energy variation, attractive or repulsive. As the BEC approaches the surface, its density profile is modulated by the standing wave formed by superposition

of incident and reflected matter waves. Due to the presence of inter-atomic interactions in a BEC, this modulation can have a dramatic effect on the reflection process. In particular, for high density BECs and low incident velocities, it triggers the formation of dynamical excitations (solitons and vortex rings) that fragment the atom cloud. Our analysis shows that although this fragmentation has no *intrinsic* effect on the reflection probability, it disperses the atoms and can therefore produce an *apparent* reduction in the reflection probability at low velocities, as observed in experiment [13]. Our calculations enable us to identify regimes in which the fragmentation of the atom cloud that accompanies low-speed quantum reflection should be either strongly enhanced or suppressed, and thereby propose new experiments to test our interpretation of the reflection process.

We consider BECs containing  $3 \times 10^5$   $^{23}\text{Na}$  atoms in a cylindrically symmetrical harmonic trap, taking the longitudinal and radial trap frequencies to be  $\omega_x = 2\pi \times 3.3$  rad s $^{-1}$  and  $\omega_r = 2\pi \times 4.5$  rad s $^{-1}$  respectively, as in experiment [13], which produce an atom cloud of equilibrium peak density  $n_0 = 2.2 \times 10^{12}$  cm $^{-3}$ . At time  $t = 0$  ms, we suddenly displace the harmonic trap by a distance  $\Delta x$  along the  $x$ -direction [13], and hence accelerate the BEC towards a region of rapid potential energy variation at  $x = \Delta x$ . We consider three different potential profiles: potential I [ $V_I(x)$ , solid curve in Fig. 1(a)] is a sharp potential step of height  $V_s = 10^{-30}$  J; potential II [ $V_{II}(x)$ , solid curve in Fig. 1(b)] is an abrupt potential drop of depth  $V_s$ ; potential III [ $V_{III}(x)$ , solid curve in Fig. 1(c)] is a model of the silicon surface, whose form is specified later. The model potentials I and II enable us to identify the key physical processes that occur when a BEC undergoes reflection, and thereby develop the understanding required to interpret experimental studies of BECs reflecting from the more complicated Si surface potential. Following the trap displacement, the total po

tential energy of each Na atom (mass  $m$ ) in the BEC is  $V_T(x, r) = V_{\text{step}}(x) + \frac{1}{2}m(\omega_x^2(x - \Delta x)^2 + \omega_r^2 r^2)$ , where  $r$  is the radial coordinate and  $V_{\text{step}}(x)$  is  $V_I(x)$ ,  $V_{\text{II}}(x)$ , or  $V_{\text{III}}(x)$ .

We determine the dynamics of the BEC in three dimensions by using the Crank-Nicolson [15] method to solve the time-dependent Gross-Pitaevskii equation [8,9]

$$i\hbar \frac{\partial \Psi}{\partial t} = \left[ -\frac{\hbar^2}{2m} \nabla^2 + V_T(x, r) + \frac{4\pi\hbar^2 a}{m} |\Psi|^2 \right] \Psi \quad (1)$$

where  $\nabla^2$  is the Laplacian in cylindrical coordinates,  $a = 2.9 \text{ nm}$  is the s-wave scattering length and  $\Psi(x, r, t)$  is the axially symmetrical condensate wavefunction at time  $t$ , normalized such that  $|\Psi|^2$  is the number of atoms per unit volume. The equilibrium density profile of the BEC in the harmonic trap is shown in Fig. 2(a).

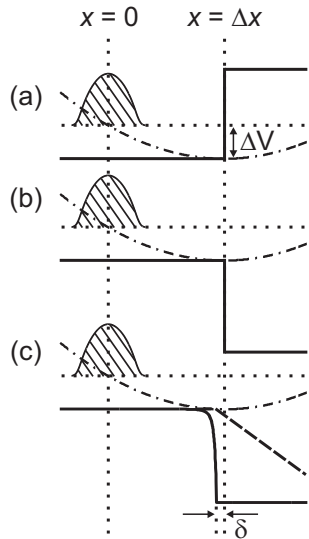


FIG. 1. Solid curves: schematic representations of  $V_I(x)$  (a),  $V_{\text{II}}(x)$  (b), and  $V_{\text{III}}(x)$  (c). Dot-dashed curves: the potential energy of the harmonic trap, shown as a function of  $x$ , immediately after the trap displacement. Shaded areas in (a)-(c) represent the initial atom density profile  $|\Psi(x, 0, 0)|^2$ . Dashed line in (c) shows the imaginary potential used to model the adsorption of Na atoms on the Si surface.

We now explore the dynamics of the BEC in potential I. When the trap is displaced at  $t = 0 \text{ ms}$ , the initial potential energy of the BEC is increased by  $\Delta V \approx \frac{1}{2}m\omega_x^2\Delta x^2$ , as shown in Fig. 1(a), causing the atoms to be incident on the potential step with a velocity  $v_x \approx \omega_x\Delta x$ . For the displacements considered here,  $\Delta V \ll V_s$ . Hence, in a classical picture, we expect the BEC to be completely reflected by the step. Figure 2 shows images of the BEC undergoing reflection from potential I after a trap displacement of  $60 \mu\text{m}$ , for which  $v_x \approx 1.2 \text{ mm s}^{-1}$ . At  $t = 90 \text{ ms}$  [Fig. 2(b)], approximately half the atoms have reached the barrier, and a standing wave has formed as a result of the superposition

of the incident and reflected waves, causing periodic modulations in the density profile. Due to the inter-atomic interactions, the high density at the peaks of the standing wave causes atoms to be pushed out from the axis of cylindrical symmetry (the  $x$ -axis), thus transferring momentum into the transverse direction. These atoms appear as the arrowed “lobes” at the top and bottom of Fig. 2(b). The lobes ride up the walls of the harmonic trap and are then reflected back towards the  $x$ -axis. This causes a cylindrically symmetrical soliton to form, which appears as the two white stripes (arrowed) in Fig. 2(c). The soliton then decays via the snake instability [18] into two vertical vortex rings, which appear as pairs of density nodes within the dashed box in Fig. 2(d). The phase of the BEC wavefunction within the dashed box in Fig. 2(d) is shown to the right of the density profile. The figure reveals a  $2\pi$  phase change around each density node, indicating quantized circulation. At the end of the oscillation, the atom cloud still contains vortex rings, and has a fragmented appearance [Fig. 3(a)]. Similar dynamics have been observed for two-dimensional BECs reflecting from a circular hard wall [10].

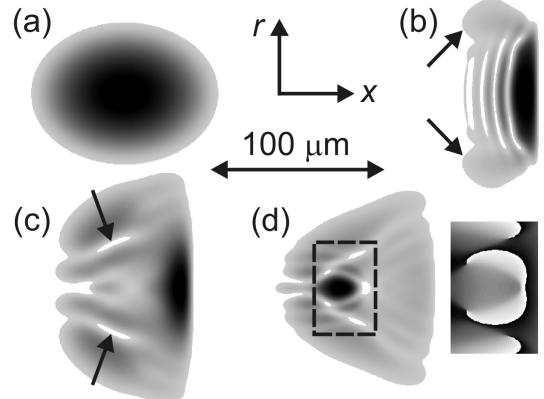


FIG. 2. Grey-scale plots of atom density (black = high) in the  $x - r$  plane (axes inset) for the BEC reflecting from potential I, shown at  $t = 0 \text{ ms}$  (a),  $90 \text{ ms}$  (b),  $122 \text{ ms}$  (c) and  $143 \text{ ms}$  (d) after a trap displacement  $\Delta x = 60 \mu\text{m}$ . The phase of the condensate wavefunction within the dashed box in (d) is shown in the grey-scale plot (white = 0, black =  $2\pi$ ) to the right of the density profile. Horizontal bar shows scale.

Our simulation for a larger trap displacement  $\Delta x = 100 \mu\text{m}$ , for which  $v_x \approx 2.1 \text{ mm s}^{-1}$ , shows very different behavior. In this case, the BEC is not disrupted by the reflection process. As shown in Fig. 3(b), the reflected atom cloud at  $t = 150 \text{ ms}$  contains no excitations and has a smooth density profile, similar to the original BEC ground state [Fig. 2(a)]. This is because, for  $\Delta x = 100 \mu\text{m}$ ,  $v_x$  is sufficiently high for the reflection process to complete before the BEC’s internal structure has time to change in response to the high density peaks in the standing wave.

We now consider quantum reflection of a BEC from the

abrupt potential drop (potential II) shown in Fig 1(b). The reflected atom clouds at  $t = 150$  ms for  $\Delta x = 60$  and  $100 \mu\text{m}$  are shown in Figs. 3(c) and (d) respectively. They are qualitatively remarkably similar to the equivalent images for potential I [Figs. 3(a) and (b)], except that they are slightly smaller because fewer atoms are reflected. When  $\Delta x = 60 \mu\text{m}$ , the reflected atom cloud has a fragmented appearance and contains a vortex ring, enclosed by the arrows in Fig. 3(c). By contrast, when  $\Delta x = 100 \mu\text{m}$  the BEC contains no excitations and has a smooth density profile [Fig. 3(d)]. This is because, just as for potential I, when  $\Delta x = 100 \mu\text{m}$  the reflection process is too fast for the BEC's internal structure to change in response to the standing wave.

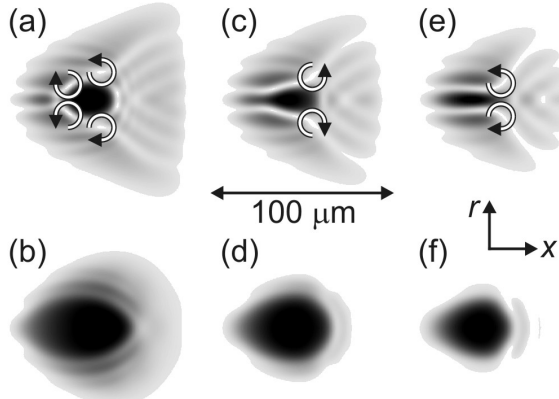


FIG. 3. Grey-scale plots of atom density (black = high) in the  $x - r$  plane (axes inset) for the BEC reflecting from potential I, shown at  $t = 150$  ms after a trap displacement  $\Delta x = 60 \mu\text{m}$  (a), and  $100 \mu\text{m}$  (b). (c) & (d) Same as (a) & (b), but for potential II. (e) & (f) Same as (a) & (b), but for potential III. Horizontal bar shows scale. Arrows in (a), (c) and (e) indicate the direction of quantized circulation around vortex cores.

Having studied two simple abrupt potential steps, we now investigate quantum reflection from a silicon surface [13] at  $x = \Delta x$ , which we model by potential III [ $V_{\text{III}}(x)$ , solid curve in Fig. 1(c)]. Potential III is based on the Casimir-Polder potential [19]

$$V_{CP}(x') = \frac{-C_4}{x'^3(x' + 3\lambda_a/2\pi^2)} \quad (2)$$

where  $C_4 = 9.1 \times 10^{-56} \text{ J m}^4$ ,  $\lambda_a = 590 \text{ nm}$  is the effective atomic transition wavelength [19], and  $x' = x - \Delta x$  is the distance from the surface. For  $x < \Delta x - \delta$ , where  $\delta = 0.2 \mu\text{m}$  is a small offset from the surface [Fig. 1(c)], we set  $V_{\text{III}}(x) = V_{CP}(x')$ . However, since  $V_{CP} \rightarrow -\infty$  as  $x \rightarrow \Delta x$ , for  $x \geq \Delta x - \delta$  we set  $V_{\text{III}}(x) = V_{CP}(\delta) + i(x - \Delta x + \delta)V_{\text{im}}$ , where  $V_{\text{im}} = 1.6 \times 10^{-26} \text{ J m}^{-1}$ . No atoms are reflected when  $x \geq \Delta x - \delta$  because the real part of  $V_{\text{III}}(x)$  is constant. The imaginary part of  $V_{\text{III}}(x)$  [dashed curve in Fig. 1(c)] models the adsorption of Na atoms by the Si surface [20]. We expect that the BEC will undergo quantum reflection when the spa-

trial variation of  $V_{\text{III}}(x)$  ensures that  $|d\lambda/dx| \gtrsim 1$  [14], where  $\lambda$  is the local de Broglie wavelength. For  $v_x = 1 \text{ mm s}^{-1}$ , the atoms are most likely to reflect  $\sim 1 \mu\text{m}$  from the surface, where  $|d\lambda/dx|$  is maximal [21].

Figures 3(e) and (f) show the reflected atom clouds at  $t = 150$  ms for  $\Delta x = 60$  and  $100 \mu\text{m}$  respectively. Although the size of the clouds is smaller than the corresponding images for potentials I and II because fewer atoms are reflected, the qualitative behavior of the BEC is the same. When  $\Delta x = 60 \mu\text{m}$ , the atom cloud is disrupted and contains a vortex ring [Fig. 3(e)], whereas for  $\Delta x = 100 \mu\text{m}$  the BEC has a smooth density profile and contains no excitations [Fig. 3(f)]. This is consistent with the experiments of Pasquini et al. [13], who observed “excited and sometimes fragmented” atom clouds following the quantum reflection of BECs incident on a silicon surface at low  $v_x$ .

To quantify how the reflection process depends on the value of  $v_x$ , and to relate our simulations to experiment [13], we made numerical calculations of the probability,  $R$ , that each atom in the BEC will quantum reflect from the Si surface potential. The solid lines in Fig. 4 show  $R$  versus  $v_x$  calculated for atom clouds with (squares) and without (crosses) inter-atomic interactions. In each case,  $R$  increases with decreasing  $v_x$ . Similar behavior was reported in Refs. [13,14,22], where  $R$  was calculated analytically in the limit  $v_x \rightarrow 0$  and numerically by solving the one-dimensional Schrödinger equation for *single atoms* reflected by the Casimir-Polder potential.

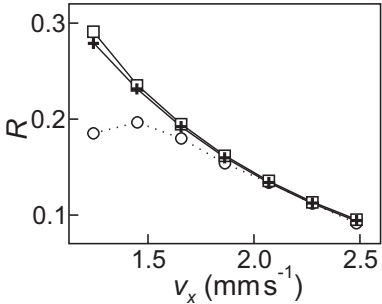


FIG. 4. Solid curves:  $R(v_x)$  for potential III, calculated from the entire reflected atom cloud with (squares) and without (crosses) inter-atomic interactions. Dotted curve with circles:  $R(v_x)$  calculated with inter-atomic interactions, but omitting regions of the atom cloud where  $|\Psi|^2 \leq 0.25 n_0$ .

A key feature of Fig. 4 is that the  $R(v_x)$  curves calculated with and without inter-atomic interactions are nearly identical, indicating that the interactions have little *intrinsic* effect on the reflection probability [23]. Consequently, inter-atomic interactions do not *immediately* explain why experimentally measured  $R$  values *decrease* with decreasing  $v_x \lesssim 1.7 \text{ mm s}^{-1}$  [13]. However, a possible explanation of this anomalous behavior does emerge when we consider how the interactions affect the structure of the atom cloud at low  $v_x$  values. In the absence of interactions, quantum reflection does not change the form

of the atom cloud. By contrast, as discussed above, interactions cause disruption and fragmentation of the atom cloud when  $v_x \lesssim 1.7 \text{ mm s}^{-1}$  (corresponding to  $\Delta x \lesssim 80 \mu\text{m}$ ): precisely the regime where anomalously low  $R$  values are observed in experiment [13]. Severe disruption of the cloud can make detection of atoms difficult in low density regions of the BEC [24], or even eject atoms from the trap [12], and hence account for the anomalously low  $R$  values observed in experiment. To simulate the effect of such losses, we recalculated  $R$  omitting the contribution from reflected atoms in low density regions of the BEC for which  $|\Psi|^2 \leq n_c$ , where  $n_c$  is a threshold below which detection of atoms can be difficult [24]. The dotted curve in Fig. 4 shows  $R(v_x)$  calculated taking  $n_c = 0.25 n_0$ . In this case, as in experiment [13], the  $R(v_x)$  curve flattens and then decreases with decreasing  $v_x \lesssim 1.7 \text{ mm s}^{-1}$ , in the regime where fragmentation of the atom cloud produces large areas of low density. We obtain qualitatively similar behavior for all values of  $n_c \gtrsim 0.1 n_0$ .

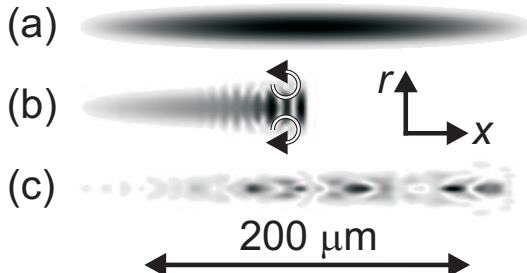


FIG. 5. Grey-scale plots of atom density (black = high) in the  $x - r$  plane (axes inset) for the BEC reflecting from potential III, shown at  $t = 0 \text{ ms}$  (a),  $150 \text{ ms}$  (b), and  $300 \text{ ms}$  (c). Horizontal bar shows scale.

The timescale on which a BEC responds to a perturbation is characterized by the correlation time, which is inversely proportional to the mean atom density [9]. We therefore expect that higher (lower) density BECs will be more (less) disrupted by the reflection process. Furthermore, the disruption should be enhanced by using lower longitudinal trap frequencies, as this increases the period of trap oscillations and hence also the reflection times. To test these predictions, we now investigate how changing the trap frequencies to  $\omega_x = 2\pi \times 1.65 \text{ rad s}^{-1}$  and  $\omega_r = 2\pi \times 15.0 \text{ rad s}^{-1}$  affects quantum reflection of the BEC from potential III. For these trap frequencies the BEC is cigar-shaped, as shown in Fig. 5(a), and  $n_0$  is almost twice that of the BEC considered above. In addition, since  $\omega_x$  is half the previous value, the reflection process proceeds more slowly for given  $\Delta x$ , and so the standing wave formed during reflection lasts longer. We accelerate the BEC towards the Si surface via a trap displacement of  $150 \mu\text{m}$ , for which  $v_x = 1.6 \text{ mm s}^{-1}$ . In this regime, the density nodes and associated  $\pi$  phase shifts that the standing wave imprints in the atom cloud during reflection lead to the formation of a chain of solitons [8,9].

At the mid-point of the first oscillation ( $t = 150 \text{ ms}$ ), several solitons [light grey stripes in Fig. 5(b)] have formed from the standing wave. Moreover, three solitons have already decayed into vortex rings, one of which is enclosed by arrows in Fig. 5(b). By the end of the oscillation at  $t = 300 \text{ ms}$  [Fig. 5(c)], many excitations have formed, causing fragmentation of the atom cloud. This extreme disruption is analogous to the explosive expansion of high density BECs following Bragg reflection in an optical lattice [8,9].

In summary, we have investigated the reflection of BECs from three abrupt potential steps, and shown that the condensate dynamics are qualitatively the same in each case. For high values of  $v_x$ , the reflection process occurs cleanly, causing almost no change in the atom density profile. But at low  $v_x$ , the standing wave formed from the superposition of the incident and reflected waves generates dynamical excitations that disrupt the atom cloud. This disruption could explain the anomalously low  $R$  values recently measured for BECs incident on a Si surface at low velocity. The fragmentation is particularly dramatic for dense slow-moving condensates, and further experiments in this regime would test our interpretation of the reflection process and the existing experiments [13]. Conversely, for low-density BECs, which are not significantly disrupted by quantum reflection, the observed values of  $R$  should continue to increase with decreasing  $v_x$ , even when  $v_x$  is small. In this regime, quantum reflection near a Si surface should provide an effective means of containing BECs and decoupling them from the surface.

We thank T. Pasquini and O. Morsch for helpful discussions.

---

- [1] M. B. Dahan *et al.*, Phys. Rev. Lett. **76**, 4508 (1996).
- [2] C. Pethick and H. Smith, *Bose-Einstein condensation in dilute gases* (Cambridge University Press, Cambridge, 2002).
- [3] O. Morsch *et al.*, Phys. Rev. Lett. **87**, 140402 (2001).
- [4] M. Andrews *et al.*, Science **275**, 637 (1997).
- [5] M.-O. Mewes *et al.*, Phys. Rev. Lett. **78**, 582 (1997).
- [6] A. Chikkatur *et al.*, Science **296**, 2193 (2002).
- [7] I. Bloch, T. Hänsch, and T. Esslinger, Phys. Rev. Lett. **82**, 3008 (1999).
- [8] R. G. Scott *et al.*, Phys. Rev. Lett. **90**, 110404 (2003).
- [9] R. G. Scott *et al.*, Phys. Rev. A. **69**, 033605 (2004).
- [10] J. Ruostekoski, B. Kneer, W. Schleich, and G. Rempe, Phys. Rev. A. **63**, 043613 (2001).
- [11] B. Wu and Q. Niu, Phys. Rev. A. **64**, 061603 (2001).
- [12] L. Fallani *et al.*, Phys. Rev. Lett. **93**, 140406 (2004).
- [13] T. Pasquini *et al.*, Phys. Rev. Lett. **93**, 223201 (2004).
- [14] F. Shimizu, Phys. Rev. Lett. **86**, 987 (2001).
- [15] D.-I. Choi and Q. Niu, Phys. Rev. Lett. **82**, 2022 (1999).

- [16] C. Raman *et al.*, Phys. Rev. Lett. **83**, 2502 (1999).
- [17] W. Hänsel, P. Hommelhoff, T. Hänsch, and J. Reichel, Nature **413**, 498 (2001).
- [18] Z. Dutton, M. Budde, C. Slowe, and L. Hau, Science **293**, 663 (2001).
- [19] H. Casimir and D. Polder, Phys. Rev. **73**, 360 (1948).
- [20] We assume that those atoms which do not quantum reflect are either adsorbed by the Si surface or undergo inelastic scattering [13].
- [21]  $|d\lambda/dx|$  becomes  $< 1$  close to the surface (for  $x' \lesssim 0.04 \mu\text{m}$  when  $v_x = 1 \text{ mm s}^{-1}$ ). Choosing  $\delta = 0.2 \mu\text{m}$  ensures that  $V_{\text{III}}(x)$  incorporates most of the reflecting region, whilst avoiding regions where the Casimir-Polder potential varies too rapidly with  $x'$  to allow accurate discretization of the wavefunction.
- [22] H. Friedrich, G. Jacoby, and C. Meister, Phys. Rev. A. **65**, 032902 (2002).
- [23] For potential II,  $R$  can be determined analytically in the absence of inter-atomic interactions by imposing the usual wavefunction matching conditions at  $x = \Delta x$ . The  $R$  values obtained in this way for a single atom are within  $\sim 5\%$  of those determined for a BEC from our numerical solution of Eq. (1): indicating that inter-atomic interactions have little effect on the  $R$  values for potential II (as shown for potential III in Fig. 4).
- [24] O. Morsch, Private communication (2004).